RSC Advances

PAPER

View Article Online
View Journal | View Issue

Cite this: *RSC Adv.*, 2021, **11**, 29786

Poly(vinylidenefluoride) polymers and copolymers as versatile hosts for luminescent solar concentrators: compositional tuning for enhanced performance†

Francesca Corsini,[a] Marco Apostolo,[b] Chiara Botta,[c] Stefano Turri[a] and Gianmarco Griffini *[a]

Novel host matrices based on fluoropolymers blended with poly(methyl methacrylate) (PMMA) are presented in this work for application in efficient and photochemically stable thin-film luminescent solar concentrators (LSCs). These systems consist of blends of PMMA with three different partially fluorinated polymers in different proportions: polyvinylidenefluoride homopolymer, a copolymer of vinylidenefluoride and chloro-trifluoro-ethylene, and a terpolymer of vinylidenefluoride, hexafluoropropylene and hydroxyl-ethyl acetate. A detailed chemical, physical and structural characterization of the obtained materials allowed us to shed light on the structure–property relationships underlying the response of such blends as a LSC component, revealing the effect of the degree of crystallinity of the polymers on their functional characteristics. An optimization study of the optical and photovoltaic (PV) performance of these fluoropolymer-based LSC systems was carried out by investigating the effect of blend chemical composition, luminophore concentration and film thickness on LSC device output. LSCs featuring copolymer/PMMA blends as the host matrix were found to outperform their homopolymer- and terpolymer-based blend counterparts, attaining efficiencies comparable to those of reference PMMA-based LSC/PV assemblies. All optimized LSC systems were subjected to weathering tests for over 1000 h of continuous light exposure to evaluate the effect of the host matrix system on LSC performance decline and to correlate chemical composition with photochemical durability. It was found that all fluoropolymer/PMMA-based LSCs outperformed reference PMMA-based LSCs in terms of long-term operational lifetime. This work provides the first demonstration of thermoplastic fluoropolymer/PMMA blends for application as host matrices in efficient and stable LSCs and widens the scope of high-performance thermoplastic materials for the PV field.

Received 11th June 2021
Accepted 5th August 2021

DOI: 10.1039/d1ra04537g

rsc.li/rsc-advances

Introduction

In the field of solar energy exploitation, luminescent solar concentrators (LSCs) have regained increasing attention in the last few years as promising technology to enable the transition towards a true integration of photovoltaics (PV) not only into the built environment,[1] but also in a variety of other fields as diverse as sensing, chemicals production, horticulture, water splitting and optical communication.[2,3] Indeed, their light weight, versatility and design flexibility in size, shape and color, together with their potential to improve the response of conventional PV systems under diffuse illumination by concentrating light without the need for bulky tracking equipment make them particularly suitable for a vast application portfolio.[2,4–6]

In their most common configurations, LSC systems can be fabricated as bulk plates or as thin films in which a transparent host matrix material contains a luminescent molecule acting as downshifting center of the incident light. Upon radiative emission of the absorbed photons by the luminophore, most of the downshifted light can be waveguided by total internal reflection towards the edges of the LSC device, where small-area PV cells collect the concentrated radiation.[7,8]

Critical to the effective wide applicability of this technology on the market is the long-term stability of the LSC device components.[9–11] In particular, it has been shown that both the

[a]*Department of Chemistry, Materials and Chemical Engineering "Giulio Natta", Politecnico di Milano, Piazza Leonardo da Vinci 32, 20133 Milano, Italy. E-mail: gianmarco.griffini@polimi.it*

[b]*Solvay Specialty Polymers, Viale Lombardia, 20, 20021 Bollate, Italy*

[c]*Institute of Sciences and Chemical Technologies "Giulio Natta" (SCITEC) of CNR, via Corti 12, 20133 Milano, Italy*

† Electronic supplementary information (ESI) available: Differential scanning calorimetry (DSC) of the pure fluoropolymer and of the fluoropolymer/PMMA blend coatings; scanning electron microscopy; X-ray diffraction (XRD) analysis; Fourier-transform infrared (FTIR) spectroscopy; fluoropolymer/PMMA blends as host matrices: optical characterization, device characterization, device architecture optimization and accelerated weathering tests. See DOI: 10.1039/d1ra04537g

photo-chemical stability of the luminescent material and the durability of the polymeric matrix play a key role in ensuring stable operational performance of the LSC assembly.[12,13] In this context, a large variety of high-efficiency luminescent systems exhibiting sufficiently good photostability have been developed.[4,14,15] This has recently led to the first large-scale demonstration of the application of LSCs in a real-life scenario.[16] Conversely, to date only few research studies have been conducted with the aim of developing suitable LSC polymeric matrices characterized by adequate optical properties and capable of ensuring satisfactory photostability.[17] Commodity amorphous polymers such as polymethyl methacrylate – PMMA – (or more generally polyacrylates) and polycarbonate (PC) are usually considered as host materials of choice because of their high transparency and appropriate refractive index, in addition to being easily processable and chemically compatible with a wide range of luminescent species.[18] Still, these systems are not free from issues associated with their outdoor durability, particularly when they are used in thin-film form. Indeed, polymer coating degradation not only may yield brittleness and opacity of the host matrix material,[19] but more importantly it may affect the waveguide process towards the edges of the device due to the formation of trap sites for the photons within the matrix, eventually limiting the efficiency of the LSC over exposure time.[20,21] Added to the impact on photon transport process, matrix degradation may also produce radical species that interact with the dye molecules, detrimentally affecting their photophysical performance (*i.e.*, photoluminescence quantum yield), or even promoting the degradation of the luminophore.[11]

To fill this gap, a large variety of alternative matrices has been recently proposed,[17] starting from intrinsically stable thermoplastic copolymers made of methyl methacrylate and styrene [poly(STY-*co*-MMA)][22] to partially fluorinated thermoset polymers[23–25] and organic–inorganic hybrid polymeric materials (*e.g.*, polysiloxane-rubber[26] and sol–gel-based hybrid ureasil systems[27]). Standing out among these, crosslinkable matrices based on partially fluorinated functional prepolymers have recently been demonstrated by our group as promising class of thermosetting host matrix materials alternative to reference host matrices (*e.g.*, PMMA) for the fabrication of highly durable polymeric waveguides for LSC devices.[12,13,23–25] In particular, both thermally- and light-induced crosslinking approaches were investigated and the resulting systems were found to be characterized by superior operational stability with respect to reference PMMA-based devices upon long-term (>1000 h) light exposure. Based on these results and on other recent demonstrations of crosslinked waveguide materials,[28] the use of thermosetting systems as host matrices for LSCs has clearly proven to be a viable approach for improved device durability. As opposed to this, examples of intrinsically stable thermoplastic polymeric systems alternative to PMMA that can ensure significantly improved outdoor durability of LSC devices are still lacking. In particular, in order to widen further the technological applicability of fluoropolymeric materials to the field of LSCs, it would be of great interest to develop new thermoplastic (melt or solution processable) fluorinated systems promoting prolonged outdoor LSC stability while maintaining the optical properties required for device application.

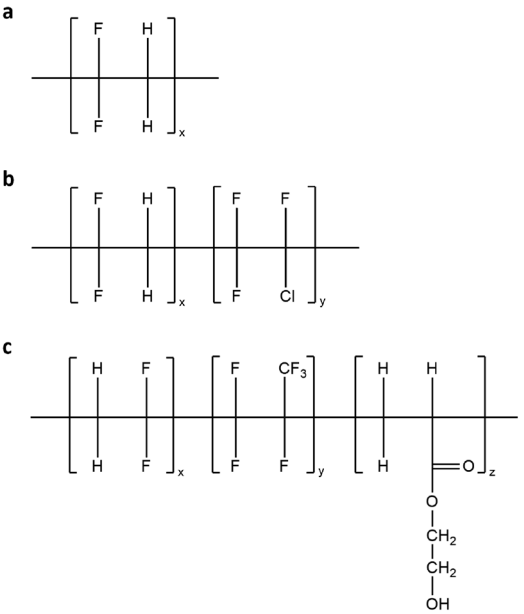

Scheme 1 (a) Pure PVDF homopolymer, (b) copolymer of VDF and chloro-trifluoro-ethylene and (c) terpolymer of VDF, hexafluoropropylene and hydroxyl-ethyl acetate.

Within this framework, a detailed investigation of novel thermoplastic fluorinated polymeric systems is presented in this work for use as host matrix materials in LSC devices (Scheme 1). The new thermoplastic formulations are based on blends of PMMA with different thermoplastic fluoropolymers based on poly(vinylidenefluoride) (PVDF), with the specific aim of reducing the crystallinity of the obtained blends which may detrimentally affect the waveguide efficiency, since crystalline domains typically act as scattering centers of the waveguided light. A thorough chemical–physical, optical and morphological characterization of these novel coating materials is presented and the effect of type and content of the blended fluoropolymer on the miscibility, optical clarity and chemical compatibility of the host matrix with a benchmark luminescent organic dye is systematically investigated. The functional performance of these fluorinated blends as host matrix materials for LSC/PV devices is evaluated at varying luminophore concentrations and coating thickness. Furthermore, a long term (>1000 h) durability study is performed under continuous light exposure on the LSC/PV devices to demonstrate the superior lifetime of the new PVDF-based luminescent systems compared to reference PMMA-based LSCs.

Results and discussion

Fluoropolymer/PMMA blends

PMMA still represents one of the most commonly employed matrix materials for the fabrication of LSC devices and its use has been extensively discussed in the literature.[17,29] PMMA-based LSC devices suffer from degradation due to the limited outdoor stability of the polymer, especially when in the form of

thin films.[12] Recent alternative systems to PMMA have been demonstrated based on the use of high-durability fluoropolymeric matrix materials. One important limitation of fluoropolymers is their intrinsically limited solubility in conventional solvents which makes it virtually impossible to blend them with other polymers or additives and imposes the use of special processing techniques for their application.[30] On the contrary, PVDF can be melt-processed on conventional extrusion and molding equipment, dissolved in polar solvents, and blended with several families of other resins. The unique properties of PVDF arise from the alternating CH_2 and CF_2 groups along the polymer backbone, which give rise to strong permanent dipoles within the polymer. The electronegativity of the geminal fluorine atoms imparts a high acidity to the adjacent hydrogen atoms. This increased hydrogen acidity allows PVDF to form homogeneous blends with several acrylate and methacrylate polymers due to hydrogen bonding interactions of the acrylic polymer carbonyl groups to CH_2 hydrogens on the PVDF chain. Similarly, this phenomenon also allows PVDF to be dissolved in polar solvents, such as *N*,*N*-dimethylacetamide, *N*-methylpyrrolidone and triethyl phosphate at room temperature. Conventional PVDF coatings are typically formulated with acrylic polymers at a PVDF/acrylic weight ratio of 70/30. This ratio has been shown to give a balance of physical properties and high exterior durability, without affecting optical properties (*viz.*, transparency).[31,32] In this work, three different grades of PVDF were investigated in blend with PMMA as potential alternative host matrices for thin film LSC devices: pure PVDF homopolymer; a copolymer of VDF and chloro-trifluoroethylene; a terpolymer of VDF, hexafluoropropylene and hydroxyl-ethyl acetate. To assess the effect of blend composition on the performance of the resulting coating, different fluoropolymer/PMMA mass ratios were tested, namely 70/30, 60/40 and 50/50.

To identify the samples, the following code has been used in this work: H*x*P*y*L*z*, C*x*P*y*L*z*, T*x*P*y*L*z* for blends of homopolymer (H), copolymer (C) or terpolymer (T) with PMMA (P) at a *x*/*y* mass ratio (with *x* and *y* referring to the wt% of fluoropolymer and PMMA, respectively), containing (when present) *z* wt% of LR305 (L).

Differential scanning calorimetry

To evaluate the compositional effect of the blends on their miscibility and their thermal transitions, differential scanning calorimetry (DSC) was performed on coatings of increasing fluoropolymer/PMMA mass ratios (the DSC curves are reported in Fig. S3 in the ESI†). As shown in Table 1, the addition of PMMA leads to an overall increase in glass transition temperature (T_g) with respect to the pristine fluoropolymer-based system, with maximum values reaching up to 70 °C, 63 °C and 62 °C in H50P50, C50P50, T50P50, respectively. The presence of a unique T_g at an intermediate value between those of the two pure components and which varies with the blend composition demonstrates the good miscibility of the fluoropolymers in PMMA. Also, the theorical T_g values were calculated using two different mathematical models: Gordon–Taylor and Kwei equations. These allow to predict the dependence of T_g on blend composition based on the free volume theory, the kinetic theory, and the thermodynamic theory.[33–37] More specifically, the Gordon–Taylor model (eqn (1)) is based on two basic assumptions: volume additivity and a linear change in volume with temperature:

$$T_{g,b} = \frac{\omega_1 T_{g,1} + k_{G-T}\omega_2 T_{g,2}}{\omega_1 + k_{G-T}\omega_2} \quad (1)$$

where $w_2 = 1 - w_1$ and the term K_{G-T} is a curve-fitting parameter whose value depends on the change in thermal expansion coefficient of each component during the glass transition and on the density of each component.[35]

Instead, the Kwei model (eqn (2)) allows to predict the T_g of polymer blends that exhibit a glass transition behavior which deviates considerably (both negatively and positively) from ideality (*e.g.*, polymer blends with S-shaped or U-shaped profiles of T_g *vs.* composition).[37,38] Indeed, in the Kwei model this deviation is interpreted as the contribution of intermolecular interactions between components in the mixture, such as hydrogen bonding. To reflect this effect, a second parameter (q) is added to the previously introduced Gordon–Taylor model:

$$T_{g,b} = \frac{\omega_1 T_{g,1} + k\omega_2 T_{g,2}}{\omega_1 + k\omega_2} + q\omega_1\omega_2 \quad (2)$$

where k (with the same physical meaning as k_{G-T}) and q are both fitting parameters.

As illustrated in Fig. 1, the experimental data obtained from DSC measurements for H/P and T/P systems show deviations with respect to the theoretical values predicted by the Gordon–Taylor model. These results may be explained by considering that fluoropolymer/PMMA blends are characterized by strong intermolecular interactions between the two components (*i.e.*, hydrogen bonds between carbonyl groups of PMMA and $-CH_2$ groups of PVDF and dipole–dipole interactions between $-CH_2$ in PMMA and $-CF_2$ in PVDF).

Conversely, the Kwei equation provides a better fit of the T_g data (higher R^2 values are indeed obtained) thanks to the extra

Table 1 Glass transition temperature (T_g), melting temperature (T_m), enthalpy of melting (ΔH_m) and degree of crystallinity (X_C) for pure homopolymer (H), copolymer (C) and terpolymer (T) systems and for O*x*P*y*, C*x*P*y* and T*x*P*y* blends

Sample	T_g [°C]	T_{melt} [°C]	ΔH_m [J g^{-1}]	X_C [%]
H	−41.4	173.0	50.8	48.6
H70P30	58.9	170.1	31.8	30.4
H60P40	63.1	166.5	25.6	24.5
H50P50	69.6	167.4	2.2	2.1
C	−27.7	168.6	18.6	17.7
C70P30	33.9	165.3	14.1	13.5
C60P40	47.2	161.0	4.3	4.1
C50P50	62.9	n.a.	n.a.	0
T	−14.4	154.3	27.2	26.0
T70P30	25.3	149.7	18.6	17.7
T60P40	40.2	n.a.	n.a.	0
T50P50	61.9	n.a.	n.a.	0

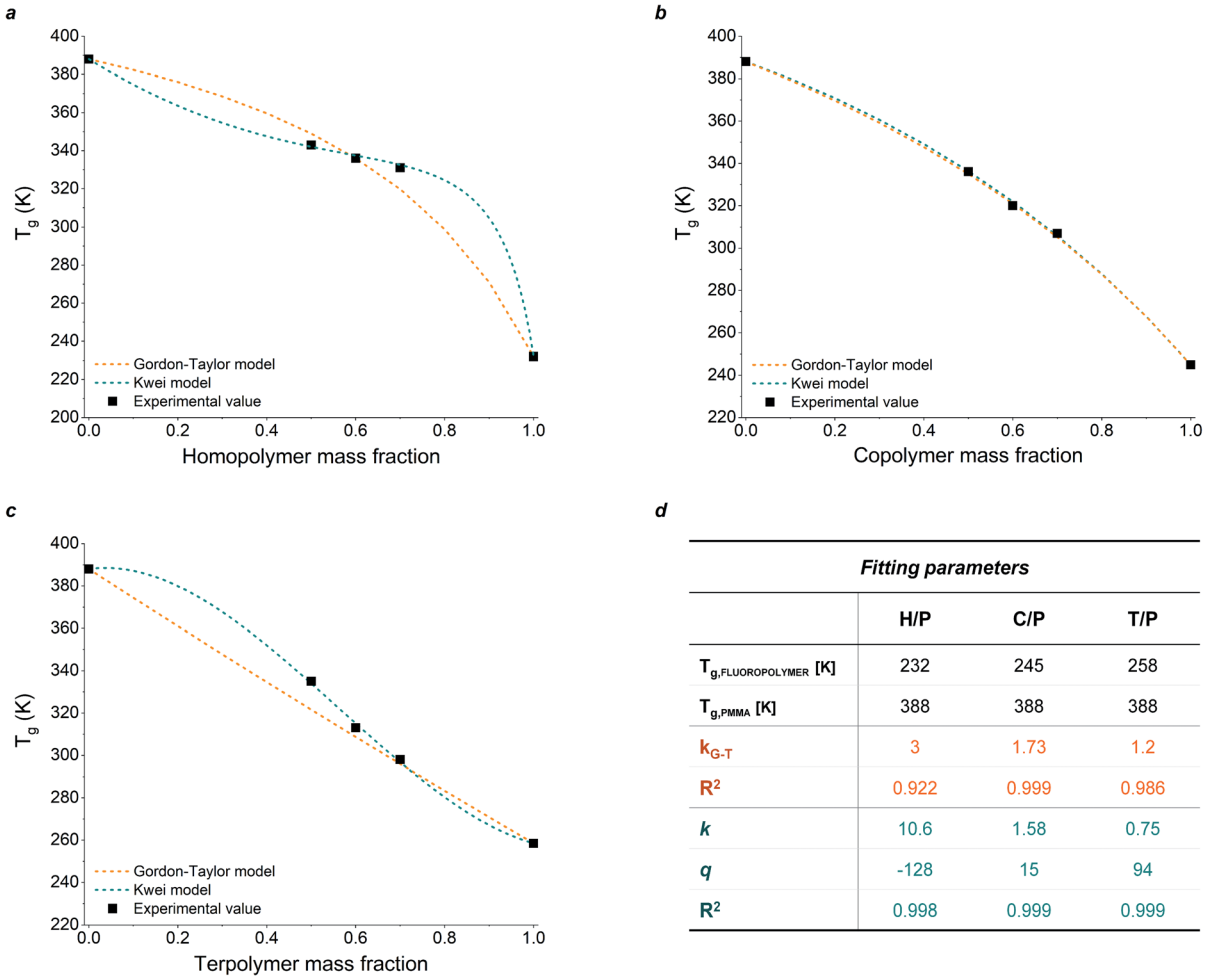

Fitting parameters			
	H/P	C/P	T/P
$T_{g,FLUOROPOLYMER}$ [K]	232	245	258
$T_{g,PMMA}$ [K]	388	388	388
k_{G-T}	3	1.73	1.2
R^2	0.922	0.999	0.986
k	10.6	1.58	0.75
q	-128	15	94
R^2	0.998	0.999	0.999

Fig. 1 Experimental and predicted T_g values of all fluoropolymer/PMMA systems as a function of the blend composition for (a) H, (b) C, (c) T. (d) Values of *k*, *q* and k_{G-T} and the goodness of fit (R^2) for fluoropolymers/PMMA blends.

fitting parameter, *q*, whose absolute value reflects the strength of the intermolecular interactions between the two components. More specifically, the higher the interactions between blend components, the stronger the rigidity of the network and therefore the more pronounced the net positive or negative deviation from ideality of T_g of the mixture. In particular, the produced S-shape composition dependence of T_g in H/P and T/P blends suggests presence of stronger intermolecular interactions between these two components with respect to C/P.[37,39,40]

In addition to a shift in T_g, a change in the degree of crystallinity X_C in the blend-based coatings was observed, the latter being defined as the ratio between the melting enthalpy of the coating ΔH_m (measured by integration of the melting peak as observed from DSC analysis) and the melting enthalpy of the fully crystalline material ΔH_0 (assumed to be equal to that of pure PVDF, 104.50 J g^{-1}),[41] as shown in eqn (3) below:

$$X_C = \frac{\Delta H_m}{\Delta H_0} \quad (3)$$

While in the fluorinated polymers X_C was found to range between 49% (for H), 26% (for T) and 18% (for C), the presence of PMMA resulted in a significant suppression of crystallinity in all fluoropolymer/PMMA blend coatings at increasing PMMA content, accompanied by a decrease in the melting temperature T_m (Table 1).

In particular, completely amorphous structures were observed for high PMMA mass ratios, namely C50P50, T60P40 and T50P50. This behaviour suggests inhibition of the growth of crystalline domains in the fluoropolymer and subsequent increase of amorphous phase upon coating formation (as verified from SEM micrographs in Fig. S4 and S5 in ESI†),[41–43] likely prospecting improved optical properties (transparency) of the corresponding coatings and possibly enhanced chemical miscibility of the luminescent dye used for LSC applications.[44]

X-ray diffraction analysis

To further investigate this effect, X-ray diffraction (XRD) analysis was conducted on spin coated samples of pure H, C, T and their corresponding blends with PMMA at different fluoropolymer/PMMA ratio (see Section S.4 in ESI†). While in pure fluoropolymer coatings the characteristic peaks associated to the non-polar PVDF α-phase were clearly distinguishable,[45,46]

a general decrease of intensity of such signals was observed by increasing PMMA content in the blend-based coatings, thus confirming a progressive suppression of PVDF crystallinity. In particular, for low fluoropolymer contents (C50P50, T60P40, T50P50), the formation of a broad band at 2Θ values between 10° and 20° was observed, characteristic of the presence of the PMMA amorphous phase.

Fourier-transform infrared spectroscopy

The effect of the presence of the amorphous phase in PMMA on the molecular characteristics of the resulting fluoropolymer/PMMA blends was also examined by means of Fourier-transform infrared (FTIR) spectroscopy. As shown in Fig. 2a, where the FTIR spectra of the H-based coatings are presented, a progressive increase in PMMA content leads to the gradual disappearance of some characteristic peaks clearly visible in the pure fluorinated polymer. In particular, a significant reduction (and ultimately a complete disappearance) in the intensity is observed for the FTIR bands at 1402 cm^{-1}, 975 cm^{-1} and 764 cm^{-1}, attributable to CH_2 stretching, CH_2 twisting and in-plane bending/rocking of the crystalline α-phase in PVDF, respectively.[47–53] Furthermore, the peak at 1382 cm^{-1} (CH_2 bending/wagging of PVDF α-phase) is also found to gradually disappear at increasing PMMA content. Concurrently, other characteristic FTIR signals are found to appear with progressively higher intensity, as a result of the incorporation of increasing amounts of PMMA in the blend-based coatings. In particular, a high intensity signal at 1728 cm^{-1} (*e.g.*, C=O stretching signal of the methacrylate group) is clearly visible for higher PMMA content, together with a broad band with a peak centered at 989 cm^{-1} (attributable to CH_3–O bending vibrations in PMMA). These observations provide an indirect rationalization of the reduction of X_C in the blend-based coatings when progressively higher PMMA mass content is incorporated, further supporting the conclusions drawn from XRD and DSC analyses. Similar trends were also reported on C- and T-based coating systems (see Section S.5 in the ESI†), thus suggesting that the mechanism for crystallization suppression is analogous in all three blend combinations explored in this work.

Thin-film luminescent solar concentrators

Optical characterization. Given the favourable chemical–physical characteristics of the fluoropolymer/PMMA-based coatings highlighted above, their potential suitability as host matrix materials for LSC applications was then investigated by imparting the optical functionality to the system through the incorporation of a commercial fluorescent dye species into the coating formulations. More specifically, perylene-based LR305 was selected as a convenient reference platform to evaluate the properties of the new host materials.

Initially, the optical response of all blend-based coatings was studied at varying fluoropolymer/PMMA wt ratios by means of UV-vis absorption spectroscopy, maintaining a constant luminophore concentration (5 wt%) with respect to PMMA which from fluorescence spectroscopy resulted to be the optimal doping level (see Fig. S8 in ESI†). The absorption intensity was found to increase linearly with the mass fraction of PMMA in the blend in accordance with the Lambert–Beer's law, that is with the dye molar concentration, thus indicating similar optical properties and good solubility of the fluorophore species in the copolymer/PMMA blends at any blend composition. Same trends were observed for homopolymer and terpolymer systems (Fig. S9 in the ESI†). Moreover, the molar extinction

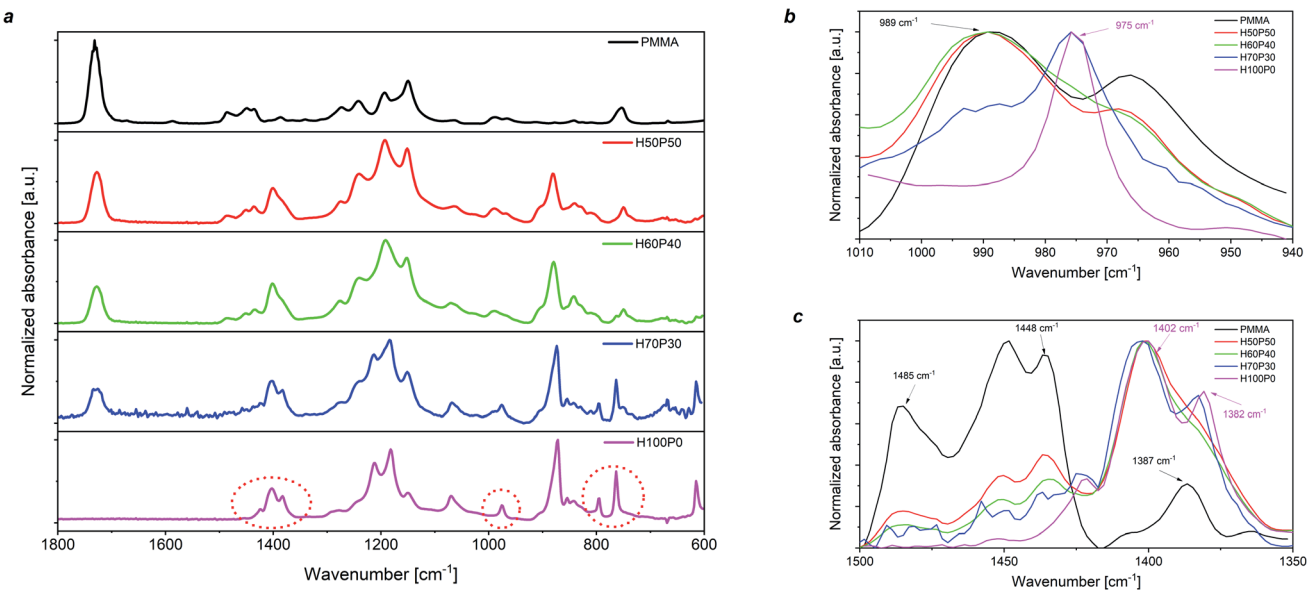

Fig. 2 (a) FTIR spectra of pure homopolymer compared with its PMMA blends. Red circles indicate some characteristic PVDF groups disappearing when PMMA content is increased. Details of FTIR spectra of pure homopolymer along with its PMMA blends in the region of (b) 1010–940 cm^{-1} and (c) 1500–1350 cm^{-1}.

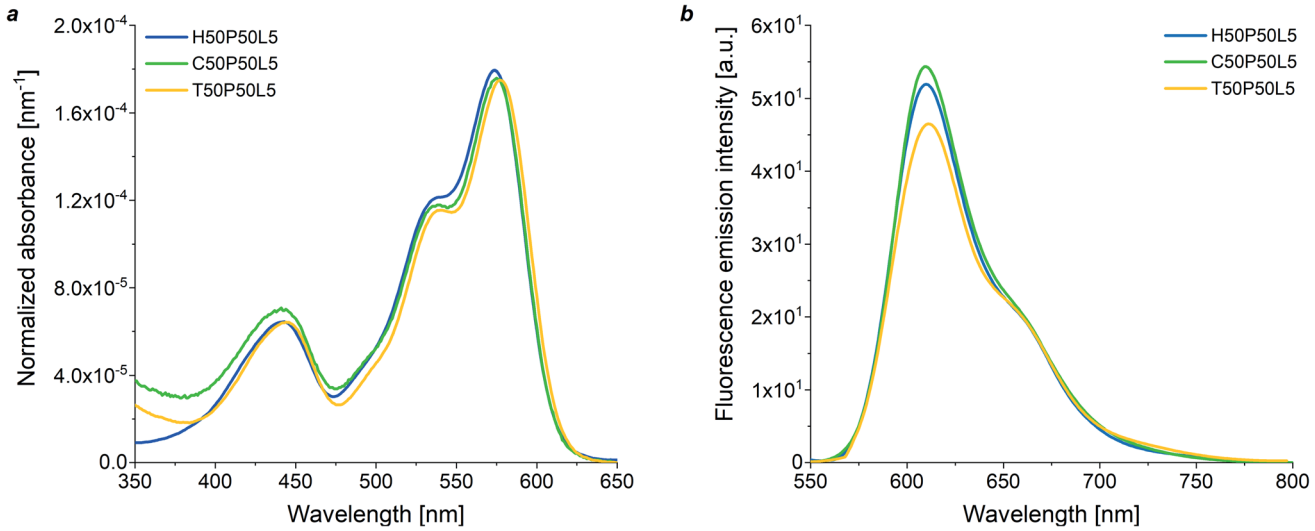

Fig. 3 (a) UV-Vis absorption spectra normalized over sample thickness and (b) front-face fluorescence emission spectra of LSC devices made of homopolymer, copolymer and terpolymer/PMMA blends host matrices at fixed weight content of both PMMA (50%) and LR305 (5% with respect to PMMA).

coefficient of the luminescent species was not found to be affected by the type of fluoropolymer present in the blend with PMMA, as evidenced by the UV-vis absorption spectra of LR305-doped 50/50 fluoropolymer/PMMA coatings (5 wt% luminophore with respect to PMMA) at constant thickness (Fig. 3a). This indicates that the same fraction of incident photons can theoretically be absorbed by the three different LR305-doped fluoropolymer/PMMA systems, thus enabling additional degrees of freedom in the selection of the host matrix.

To gain further insights into the optical properties of fluoropolymer/PMMA blends, fluorescence emission spectroscopy was also performed (Fig. S10 in the ESI†). Fig. 3b shows the fluorescence emission spectra of dye-doped 50/50 fluoropolymer/PMMA blends at fixed luminophore content (5 wt%). The C50P50L5 system was found to exhibit a slightly higher fluorescence intensity as compared with H50P50L5 and T50P50L5 blends, despite their similar absorption profile. This could be ascribed to the higher degree of crystallinity shown by H and T-based systems, which might cause a reduction in the solubility of the fluorophore species, formation of aggregates and partial fluorescence quenching.

LSC/PV device characterization

Based on the optical characterization of the new fluoropolymer/PMMA blend systems as host matrix materials in LSC devices, an optimization of the main LSC device parameters (dye concentration, blend composition and LSC thin film thickness) was carried out on both LSCs as photonic systems and LSC/PV-cell assemblies as photovoltaic systems by evaluating their external and internal efficiency (η_{ext}, η_{int}) and their optical photovoltaic efficiency ($\eta_{LSC\text{-}PV}$), respectively. These figures of merit are defined in Section S.7 in ESI.†

The effect of luminophore concentration (3 wt%, 5 wt%, 7 wt%, 10 wt% with respect to PMMA) on the performance of LSC systems based on fluoropolymer/PMMA = 50/50 blends was first investigated. η_{ext} and $\eta_{LSC\text{-}PV}$ were found to reach a maximum value at 5 wt% LR305 concentration in every system considered (see Fig. S11 and Table S2 in the ESI†). Above 5 wt%, a general decrease in LSC performance was observed. This trend might be ascribed to the presence of dissipative processes such as fluorescence quenching (due to either reabsorption events or dye aggregation) which become more prominent for higher dye concentrations.[54,55] Moreover, C/P blends were found to be more performing than the corresponding H/P and T/P counterparts. These findings are in close agreement with fluorescence emission spectroscopic analysis and further corroborate the previous hypothesis according to which the higher degree of crystallinity shown by H/P and T/P systems may yield fluorescence attenuation owing to the reduction of photon transport efficiency within the waveguide material.

The effect of coating thickness on η_{ext}, η_{int} and $\eta_{LSC\text{-}PV}$ of the fluoropolymer/PMMA blends-based LSC systems was also studied by varying the polymer-matrix-to-solvent ratio and the spin-coating speed. As shown in Fig. 4a–c, a higher film thickness led to an increase in LSC performance likely due to a higher amount of fluorophore species within the coating. In particular, an increase of ~35% in η_{ext} and $\eta_{LSC\text{-}PV}$, was detected when going from 1.0 μm to 3.2 μm thick luminescent coatings (see also Table S3 in the ESI†). Thicker LSC films could not be obtained due to worsening of the surface quality of the films (spin coating speeds lower than 300 rpm and polymer : solvent ratios higher than 10 : 90 both led to very rough and inhomogeneous LSC films), in turn causing a decrease in the waveguiding efficiency of the polymeric host matrix as evidenced by the sharp decrease in η_{int} (see Fig. 4e).

Finally, the effect of blend composition (fluoropolymer/PMMA = 50/50, 60/40 and 70/30 wt. ratio) on LSC and LSC-PV device performance was also examined, as reported in Fig. 4d–f (numerical results are reported in Table S4 in ESI,†

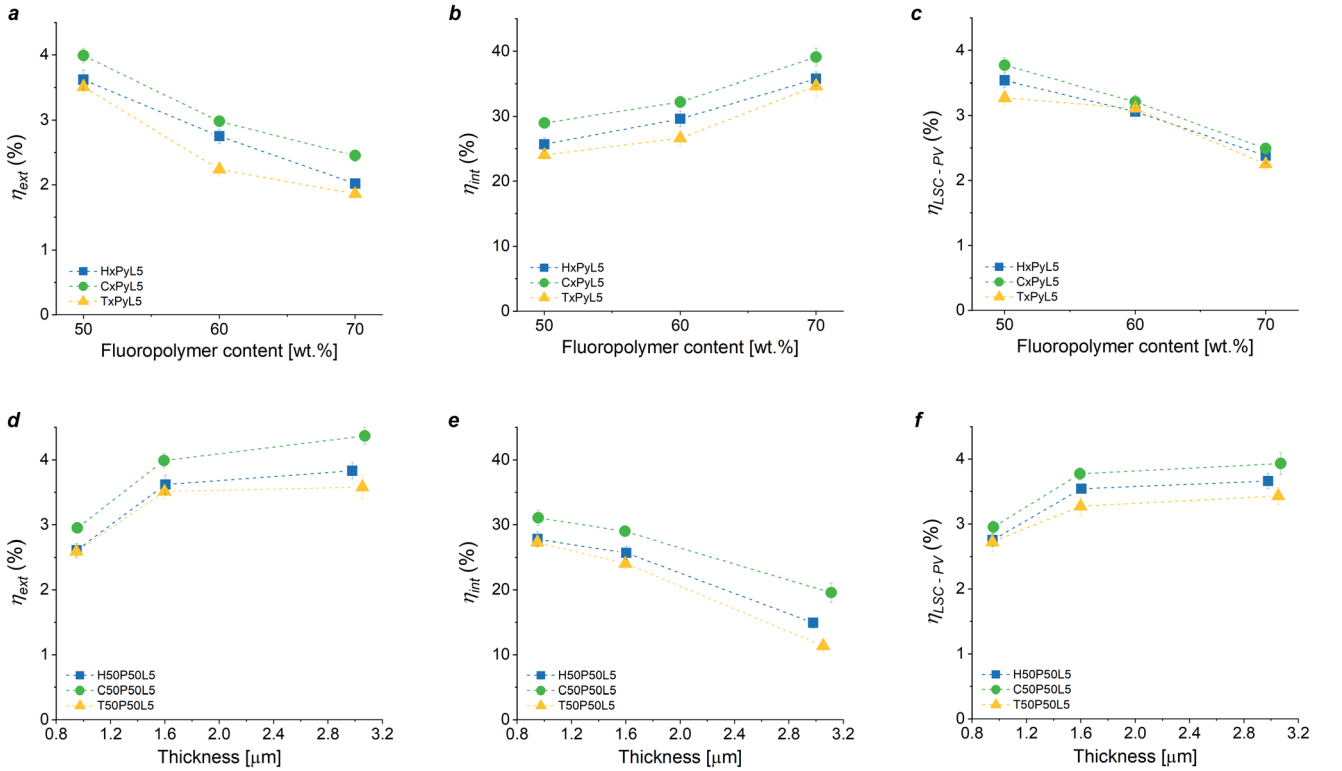

Fig. 4 (a) η_{ext}, (b) η_{int} and (c) η_{LSC-PV} *versus* fluoropolymer content for homopolymer, copolymer and terpolymer blends with PMMA. The concentration of organic dye was kept constant at 5% weight with respect to PMMA. (d) η_{ext}, (e) η_{int} and (f) η_{LSC-PV} *versus* thickness for C50P50L5, H50P50L5, T50P50L5 systems. The thickness of the LSC films was varied by changing the polymer matrix to solvent weight ratio or the spin coating speed.

where also values for the concentration factor C are reported). In general, an increase in fluoropolymer content from 50 wt% to 70 wt% resulted in a ~30% drop in LSC performance in terms of both η_{ext} and η_{LSC-PV}, and in an enhancement of η_{int} irrespective of the chemical nature of the fluoropolymer used in the blend, owing to the decrease in the effective luminophore content as the fluoropolymer/PMMA ratio is increased. In particular, C/P blend systems were systematically found to perform better than H/P and T/P LSCs in all ranges of fluoropolymer/PMMA proportions explored. This trend can be associated to the semi-crystalline nature of the blends and its effect on the optical properties (clarity) of the coatings and on the level of luminophore solubility in the polymer matrix. Furthermore, it is worth noticing that copolymer-based devices at low fluoropolymer content (50% and 60% weight concentration, C50P50L5 and C60P40L5) were proven to be comparable in terms of PV performance to benchmark PMMA-based LSC counterparts (see Section S8 in ESI†). This further corroborates the potential of this class of thermoplastic blends as readily accessible platform alternative to PMMA to fabricate fully operating LSC devices.

Accelerated weathering tests

The photo-oxidation of polymeric host matrix materials is one of the main bottlenecks of organic-based LSCs since it detrimentally affects the waveguiding process during LSC operation under continuous illumination. Consequently, an accurate study of the long-term outdoor durability of the new fluoropolymer/PMMA blend systems is necessary to prove their factual viability as novel stable and performing host matrices. To this end, accelerated weathering tests were conducted on LSC/PV-cell assemblies based on optimized C/P blends (C50P50L5, C60P40L5, C70P30L5) and their response was compared with pure PMMA-based LSCs used as reference devices (details in the Experimental section).

The weathering behaviour of the LSC devices was studied by analysing their PV response during prolonged light exposure. As can be observed in Fig. 5a, a general decrease in performance was found for reference PMMA-based LSC devices, which exhibited an over 30% loss of their initial η_{LSC-PV} after 1000 h. On the contrary, during the same aging test all C/P-based LSCs were found to fully retain their initial PV response. These trends were found to be in close agreement with the optical response (fluorescence) of the same coatings prior to and after prolonged light exposure Fig. 5b.

Interestingly, an initial increase in η_{LSC-PV} was detected in fluoropolymer-based systems, as opposed to PMMA-based devices. A similar trend was already observed in other cross-linked[56–58] and/or fluorinated[11,12,24] polymeric matrices previously proposed in the literature. Although still under investigation, this surprising behaviour could be correlated with the rapid formation of a non-fluorescent radical anion form of the perylene species upon irradiation in the presence of

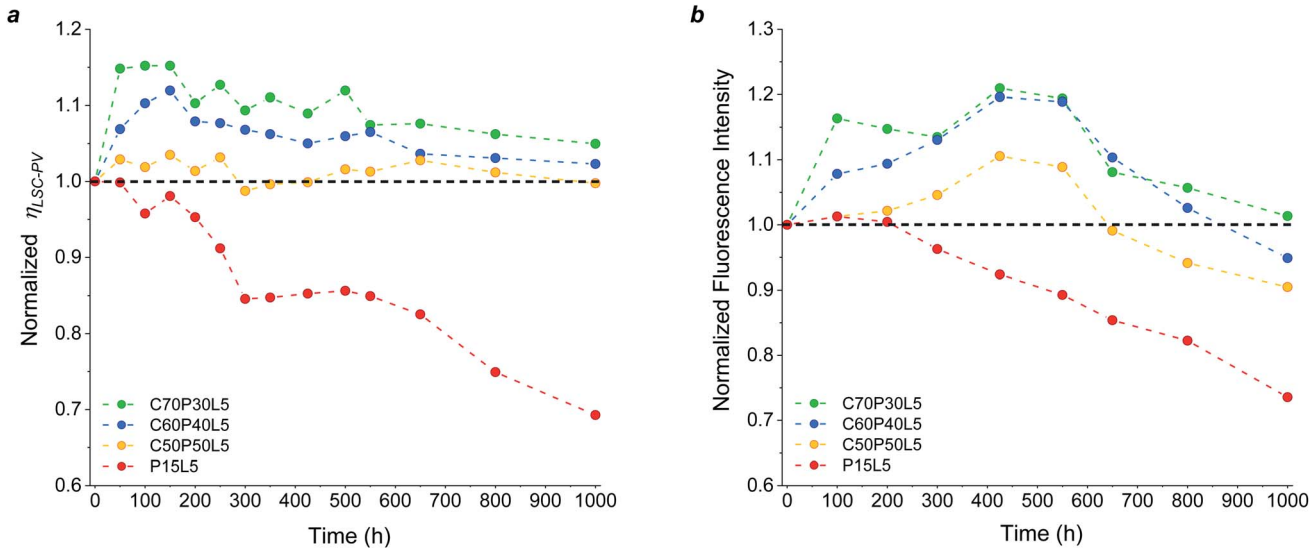

Fig. 5 (a) Normalized P_{LSC-PV} (bottom) *versus* time of exposure for copolymer/PMMA host matrix systems at different PVDF content and pure PMMA. (b) Normalized fluorescence emission intensity *versus* exposure time for PVDF-based systems and PMMA as reference (excitation wavelength 445 nm).

UV light, which persists in anaerobic conditions. In the presence of high-electron-affinity oxidizing moieties such as oxygen, this radical anion is quickly oxidized to its initial form *via* an electron-transfer reaction upon which fluorescence is recovered and the performance of the LSC device is restored.[57–62]

Finally, FTIR spectroscopy analysis was performed to assess the molecular modifications occurring to the system during light exposure and to correlate them to the observed PV trends. To this end, the evolution of the FTIR spectrum of PMMA-based samples was monitored at increasing light exposure time (0 h, 500 h and 1000 h) (Fig. S15a in ESI†). After long-term exposure the intensity of the characteristic peaks attributed to the organic dye was found to decrease sharply, likely indicating a possible degradation of its lateral substituents, according to a mechanism previously proposed in the literature.[11] Moreover, prolonged light exposure on PMMA-based LSC systems led to the appearance of two bands in the carbonyl region adjacent to the main acrylate C=O stretching peak that may be attributed to the formation of oxidation products in the dye molecule and in the polymeric matrix. As opposed to PMMA-based LSC devices and in agreement with LSC device results presented earlier, no significant modifications to the FTIR spectra of fluoropolymer-based blends were found upon prolonged light exposure (Fig. S14b in ESI†), thus further confirming their excellent photochemical stability.

Experimental

Materials

All materials employed in this study are of commercial source and were used as received. Lumogen F Red 305 (from now on referred to as LR305, BASF) was used as the fluorescent doping species in all polymeric coatings presented in this work. PMMA (Perspex XT, Lucite) was used as polymeric carrier in reference luminescent coatings. Solef 6010 poly(vinylidenefluoride) – PVDF, Solef 31508 (a poly(vinylidenefluoride-*co*-chlorotrifluoroethylene) copolymer), and Solef 11005 (a poly(vinylidenefluoride-*co*-hexafluoropropylene-*co*-hydroxyethylacrylate) terpolymer) were produced and supplied by Solvay Specialty Polymers. Chloroform ($CHCl_3$), toluene and *N*-methylpyrrolidone (NMP) were purchased by Sigma Aldrich and used as solvents for the fabrication of LSC devices.

Characterization

UV-vis absorption spectra were recorded by means of a Jasco V-570 UV-VIS-NIR Spectrophotometer in transmission mode. Fluorescence emission spectra were collected on a Jasco FP-6600 Spectrofluorometer with λ_{exc} = 445 nm. FTIR spectra were acquired on a Nicolet 760-FTIR Spectrophotometer. Spin-coating (WS-400B-NPP Spin-Processor, Laurell Technologies Corporation) technology was used to prepare solid state samples deposited onto glass/quartz/KBr substrates for UV-vis, fluorescence and FTIR spectroscopic analyses. The coating thickness was measured by optical profilometry (Filmetrics Profilm3D). Differential scanning calorimetry (DSC) was performed using a Mettler-Toledo DSC/823e instrument in nitrogen environment and at a scan rate of 20 °C min^{-1}. Bruker D8 Advance instrument was used to perform X-ray Diffraction (XRD) analysis. Scanning electron microscopy (SEM) micrographs was acquired with a Carl Zeiss EVO 50 Extended Pressure at an accelerating voltage of 15.00–17.50 kV.

PLQYs of films were obtained by using a homemade integrating sphere, as previously reported.[63]

To collect the spectrally-resolved optical power output spectra of the considered thin-film LSCs, the systems top face was illuminated with an Abet Technologies Sun 2000 solar simulator, equipped with an AM 1.5 filter and calibrated to 1 Sun (irradiance of 1000 ± 10 W m^{-2}). Meanwhile,

a spectroradiometer (International Light Technologies ILT950) equipped with a cosine corrector was positioned at the center of the edge, while the other edges were covered with black tape. The optical power output spectra of the LSCs were recorded using SpectrILight III software. From these, the internal and external photon efficiencies were calculated. Current–voltage (*I–V*) curves of LSC/PV-cell assemblies were recorded using LabView software. A Keithley 2612 digital multimeter source-measuring unit allowed to perform the voltage scans and measure the current output. upon AM 1.5 G solar illumination at 1000 W m^{-2}. In the experimental setup, an absorbing black backdrop was placed in contact with the LSC posterior side to avoid photocurrent overestimation due to photon double-pass effects and a black mask was positioned on the frontal face of the LSC system to prevent direct illumination of the PV cells.

LSC/PV-cell assemblies were subjected to accelerated aging tests in a weather-o-meter chamber (Solarbox 3000e, Cofomegra S.r.l.) under continuous Xenon light illumination for the entire duration of the test (>1000 h). The instrument was equipped with a filter cutting all wavelengths below 280 nm. The total irradiance was measured by means of a ILT950 spectroradiometer connected with a cosine corrector and found to be approximately 1000 W m^{-2} (see the irradiation spectrum in Fig. S14 in ESI†). A constant relative humidity (20%) and a fixed working temperature (45 °C) were maintained inside the testing chamber. To monitor the performance of the LSC devices during accelerated aging tests, their PV response together with the fluorescence spectra were recorded over time.

Device fabrication

For the preparation of LSCs based on fluoropolymer/PMMA blends, the considered fluoropolymer was dissolved under magnetic stirring at 80 °C in a given amount of NMP (depending on PMMA/fluoropolymer mass ratio), thereby forming the base solution. In parallel, another solution (the luminescent solution) was prepared mixing a fixed amount of PMMA and LR305 with toluene in a flask for 6 h holding the temperature at 80 °C. The total solid concentration (PMMA + fluoropolymer) was fixed to 10 wt% in solvent. The luminescent solution was added to the base solution and the obtained blend was left under stirring at 80 °C overnight to achieve complete mixing. After that, the solution was deposited onto glass substrates by spin coating (1200 rpm, 40 s) to obtain the LSC thin films. The as-cast samples were subjected to an annealing step into a vacuum oven at 220 °C for 5 min to ensure complete solvent evaporation. Reference PMMA-based LSC systems were prepared starting from a 10 wt% solution of solid PMMA in $CHCl_3$. An amount of LR305 corresponding to 5 wt% with respect to PMMA weight was added to achieve the same optical density found in the fluoropolymer-based LSCs. The same spin coating conditions were maintained. All LSC devices were fabricated on glass substrates (50 mm × 50 mm × 6 mm).

The fabrication of the LSC-PV assembly was performed by edge-coupling IXOLAR monocrystalline high efficiency silicon solar cells (IXYS IXOLAR SolarBIT KXOB22-12X1F, active area 2.2 × 0.6 cm^2, $V_{OC} = 0.64 \pm 0.01$ V, $J_{SC} = 42.60 \pm 0.42$ mA cm^{-2}, FF = 69.4 ± 0.3%, power conversion efficiency = 18.69 ± 0.23%). Norland index matching liquid 150 (refractive index 1.52) was used as optical coupling agent. LSCs were attached to two modules, each incorporating two monocrystalline silicon PV cells connected in series so that two opposite edges of the LSC glass substrate faced the photoactive area of one PV module each.

Conclusions

Novel high-durability thermoplastic systems based on blends of partially fluorinated polymers and PMMA were presented in this work for application as thermoplastic host matrix materials in thin-film LSC devices. A detailed chemical, structural and morphological characterization of these new fluoropolymer/PMMA blends evidenced their favorable chemical, physical and optical properties. The functional performance of the new fluoropolymer/acrylic blends as host matrices in LSC/PV assemblies was evaluated. A detailed analysis of the main device parameters (dye concentration, chemical composition of the blend and film thickness) showed that the fluoropolymer/PMMA relative proportions in the luminescent coating have a strong effect on the performance of the resulting LSC/PV, leading to output performance comparable to that obtained on benchmark PMMA-based LSC/PV devices. To assess the long-term photochemical stability of the new fluorinated systems, prolonged weathering tests (>1000 h) were conducted on optimized LSC/PV devices. Systems based on fluoropolymer/PMMA blends exhibited exceptionally stable device response throughout the test with minimal performance loss even over 1000 h of continuous white-light illumination. Conversely, reference PMMA-based LSC/PV devices displayed an overall ~30% performance loss in the same time frame. As demonstrated by FTIR results, the improved long-term stability of LSC based on fluoropolymer blends could be attributed to their intrinsic photochemical stability, which in turn prevents the occurrence of radical-induced photodegradation phenomena in the dye molecule during light exposure.

To our knowledge, the present work represents the first example of LSC systems based on thermoplastic fluorinated polymers as host matrices, and provides further evidence of the potential of this class of highly performing materials as accessible platform alternative to PMMA to fabricate LSC devices with excellent long-term operational response while preserving efficiency.

Conflicts of interest

The authors declare that they have no known competing financial interests or personal relationships that could have appeared to influence the work reported in this paper.

References

1 F. Meinardi, F. Bruni and S. Brovelli, *Nat. Rev. Mater.*, 2017, **2**, 1–9.

2 L. Ceccherini Nelli and G. Gallo Afflitto, in *Sustainable Building for a Cleaner Environment: Selected Papers from the World Renewable Energy Network's Med Green Forum 2017*, ed. A. Sayigh, Springer International Publishing, Cham, 2019, pp. 327–334.
3 G. Panzeri, E. Tatsi, G. Griffini and L. Magagnin, *ACS Appl. Energy Mater.*, 2020, **3**, 1665–1671.
4 I. Papakonstantinou, M. Portnoi and M. G. Debije, *Adv. Energy Mater.*, 2021, **11**, 1–13.
5 A. Reinders, R. Kishore, L. Slooff and W. Eggink, *Jpn. J. Appl. Phys.*, 2018, **57**, 1–10.
6 J. ter Schiphorst, M. L. M. K. H. Y. K. Cheng, M. van der Heijden, R. L. Hageman, E. L. Bugg, T. J. L. Wagenaar and M. G. Debije, *Energy and Buildings*, 2020, **207**, 27–30.
7 M. Rafiee, S. Chandra, H. Ahmed and S. J. McCormack, *Opt. Mater.*, 2019, **91**, 212–227.
8 G. Griffini, M. Levi and S. Turri, *Renewable Energy*, 2015, **78**, 288–294.
9 I. Baumberg, O. Berezin, A. Drabkin, B. Gorelik, L. Kogan, M. Voskobojnik and M. Zaidman, *Polym. Degrad. Stab.*, 2001, **73**, 403–410.
10 J. M. Delgado-Sanchez, *Sol. Energy Mater. Sol. Cells*, 2019, **202**, 110134.
11 G. Griffini, L. Brambilla, M. Levi, M. Del Zoppo and S. Turri, *Sol. Energy Mater. Sol. Cells*, 2013, **111**, 41–48.
12 G. Griffini, M. Levi and S. Turri, *Sol. Energy Mater. Sol. Cells*, 2013, **118**, 36–42.
13 G. Griffini and S. Turri, *J. Appl. Polym. Sci.*, 2016, **133**, 1–16.
14 S. Mattiello, A. Sanzone, F. Bruni, M. Gandini, V. Pinchetti, A. Monguzzi, I. Facchinetti, R. Ruffo, F. Meinardi, G. Mattioli, M. Sassi, S. Brovelli and L. Beverina, *Joule*, 2020, **4**, 1988–2003.
15 B. McKenna and R. C. Evans, *Adv. Mater.*, 2017, **29**, 1606491.
16 Á. Bognár, S. Kusnadi, L. H. Slooff, C. Tzikas, R. C. G. M. Loonen, M. M. de Jong, J. L. M. Hensen and M. G. Debije, *Renewable Energy*, 2020, **151**, 1141–1149.
17 G. Griffini, *Frontiers in Materials*, 2019, **6**, 29.
18 M. Zettl, O. Mayer, E. Klampaftis and B. S. Richards, *Energy Technol.*, 2017, **5**, 1037–1044.
19 J. R. White, *C. R. Chim.*, 2006, **9**, 1396–1408.
20 Y. Li, X. Zhang, Y. Zhang, R. Dong and C. K. Luscombe, *J. Polym. Sci., Part A: Polym. Chem.*, 2019, **57**, 201–215.
21 I. Papakonstantinou and C. Tummeltshammer, *Optica*, 2015, **2**, 841.
22 A. F. Mansour, H. M. A. Killa, S. A. El-wanees and M. Y. El-sayed, *Polym. Test.*, 2005, **24**, 519–525.
23 E. Tatsi and G. Griffini, *Sol. Energy Mater. Sol. Cells*, 2019, **196**, 43–56.
24 G. Griffini, M. Levi and S. Turri, *Prog. Org. Coat.*, 2014, **77**, 528–536.
25 D. Pintossi, A. Colombo, M. Levi, C. Dragonetti, S. Turri and G. Griffini, *J. Mater. Chem. A*, 2017, **5**, 9067–9075.
26 M. Buffa, S. Carturan, M. G. Debije, A. Quaranta and G. Maggioni, *Sol. Energy Mater. Sol. Cells*, 2012, **103**, 114–118.
27 A. Kaniyoor, B. Mckenna, S. Comby and R. C. Evans, *Adv. Opt. Mater.*, 2016, **4**, 444–456.
28 I. Meazzini, C. Blayo, J. Arlt and A. Marques, *Mater. Chem. Front.c*, 2017, **1**, 2271–2282.
29 W. G. J. H. M. van Sark, K. W. J. Barnham, L. H. Slooff, A. J. Chatten, A. Büchtemann, A. Meyer, S. J. McCormack, R. Koole, D. J. Farrell, R. Bose, E. E. Bende, A. R. Burgers, T. Budel, J. Quilitz, M. Kennedy, T. Meyer, C. D. M. Donegá, A. Meijerink and D. Vanmaekelbergh, *Opt. Express*, 2008, **16**, 21773.
30 H. Teng, *Appl. Sci.*, 2012, **2**, 496–512.
31 S. R. Gaboury and K. A. Wood, *Surf. Coat. Int., Part B*, 2002, **85**, 295–300.
32 Y. Li, G. Zhang, S. Song, H. Xu, M. Pan and G. J. Zhong, *Polymers*, 2017, **9**, 1–18.
33 W. Brostow, R. Chiu, I. M. Kalogeras and A. Vassilikou-Dova, *Mater. Lett.*, 2008, **62**, 3152–3155.
34 P. R. Couchman, *Macromolecules*, 1978, **11**, 1156–1161.
35 M. Gordon and J. S. Taylor, *Rubber Chem. Technol.*, 1953, **26**, 323–335.
36 J. M. Gordon, G. B. Rouse, J. H. Gibbs and W. M. Risen, *J. Chem. Phys.*, 1977, **66**, 4971–4976.
37 T. K. Kwei, *J. Polym. Sci., Polym. Lett. Ed.*, 1984, **22**, 307–313.
38 R. Pinal, *Entropy*, 2008, **10**, 207–223.
39 S. W. Kuo and H. T. Tsai, *Macromolecules*, 2009, **42**, 4701–4711.
40 L. Weng, R. Vijayaraghavan, D. R. MacFarlane and G. D. Elliott, *Cryobiology*, 2014, **68**, 155–158.
41 J. Cheng, J. Zhang and X. Wang, *J. Appl. Polym. Sci.*, 2013, **127**, 3997–4005.
42 I. S. Elashmawi and N. A. Hakeem, *Polym. Eng. Sci.*, 2008, **48**, 895–901.
43 W. Fan and S. Zheng, *J. Polym. Sci., Part B: Polym. Phys.*, 2007, **45**, 2580–2593.
44 F. Ciardelli, G. Ruggeri and A. Pucci, *Chem. Soc. Rev.*, 2013, **42**, 857–870.
45 R. Gregorio, *J. Appl. Polym. Sci.*, 2006, **100**, 3272–3279.
46 M. Li, H. J. Wondergem, M. J. Spijkman, K. Asadi, I. Katsouras, P. W. M. Blom and D. M. De Leeuw, *Nat. Mater.*, 2013, **12**, 433–438.
47 S. Mohamadi, in *Infrared Spectroscopy – Materials Science, Engineering and Technology*, ed. Theophile Theophanides, IntechOpen, 2012, pp. 213–232.
48 P. Nallasamy and S. Mohan, *Indian J. Pure Appl. Phys.*, 2005, **43**, 821–827.
49 M. Sharma, K. Sharma and S. Bose, *J. Phys. Chem. B*, 2013, **117**, 8589–8602.
50 Z. Yin, B. Tian, Q. Zhu and C. Duan, *Polymers*, 2019, **11**, 2033.
51 X. Cai, T. Lei, D. Sun and L. Lin, *RSC Adv.*, 2017, **7**, 15382–15389.
52 S. Golcuk, A. E. Muftuoglu, S. U. Celik and A. Bozkurt, *J. Polym. Res.*, 2013, **20**, 144.
53 M. Kobayashi, K. Tashiro and H. Tadokoro, *Macromolecules*, 1975, **8**, 158–171.
54 K. A. Colby, J. J. Burdett, R. F. Frisbee, L. Zhu, R. J. Dillon and C. J. Bardeen, *J. Phys. Chem.*, 2010, **114**, 3471–3482.
55 C. Haines, M. Chen and K. P. Ghiggino, *Sol. Energy Mater. Sol. Cells*, 2012, **105**, 287–292.

56 G. Fortunato, E. Tatsi, F. Corsini, S. Turri and G. Griffini, *ACS Appl. Polym. Mater.*, 2020, **2**, 3828–3839.
57 L. A. F. Vingerhoets, J. ter Schiphorst, W. R. Hagen and M. G. Debije, *Sol. Energy*, 2019, **189**, 314–317.
58 I.-S. Shin, T. Hirsch, B. Ehrl, D.-H. Jang, O. S. Wolfbei and J.-I. Hong, *Anal. Chem.*, 2012, **84**, 9163–9168.
59 N. Tanaka, N. Barashkov, J. Heath and W. N. Sisk, *Appl. Opt.*, 2006, **45**, 3846–3851.
60 R. O. Marcon and S. Brochsztain, *J. Phys. Chem. A*, 2009, **113**, 1747–1752.
61 E. R. Draper, R. Schweins, R. Akhtar, P. Groves, V. Chechik, M. A. Zwijnenburg and D. J. Adams, *Chem. Mater.*, 2016, **28**, 6336–6341.
62 E. R. Draper, J. J. Walsh, T. O. McDonald, M. A. Zwijnenburg, P. J. Cameron, A. J. Cowan and D. J. Adams, *J. Mater. Chem. C*, 2014, **2**, 5570–5575.
63 J. Moreau, U. Giovanella, J. P. Bombenger, W. Porzio, V. Vohra, L. Spadacini, G. Di Silvestro, L. Barba, G. Arrighetti, S. Destri, M. Pasini, M. Saba, F. Quochi, A. Mura, G. Bongiovanni, M. Fiorini, M. Uslenghi and C. Botta, *ChemPhysChem*, 2009, **10**, 647–653.